Geochemistry of detrital magnetite as a provenance tool in Alaska's Yukon-Tanana Upland

Robert G. McDermott[1]*, Douglas C. Kreiner[1], James V. Jones III[1], Sean P. Regan[2]

[1]U.S. Geological Survey, Alaska Science Center, Anchorage, AK, [2]Department of Geosciences, University of Alaska Fairbanks, Fairbanks, AK

*corresponding author: rmcdermott@usgs.gov

1. Introduction

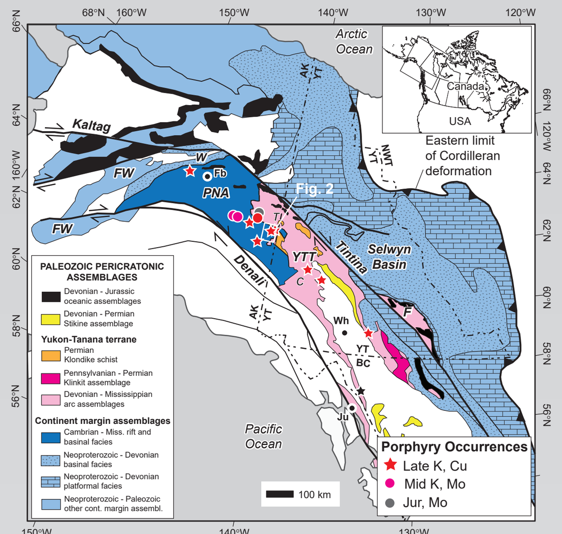

Figure 1: Northern Cordillera terrane framework and porphyry deposits. T-Taurus porphyry Cu-Mo(-Au). Adapted from Murphy et al. (2006) and Kreiner et al. (2020 and 2023).

Motivation

Develop detrital magnetite geochemistry and (U-Th)/He thermochronometry as a tool for tracking porphyry systems in the Northern Cordillera, with the Taurus porphyry Cu-Mo(-Au) deposit as a test case

2. Study area and sampling

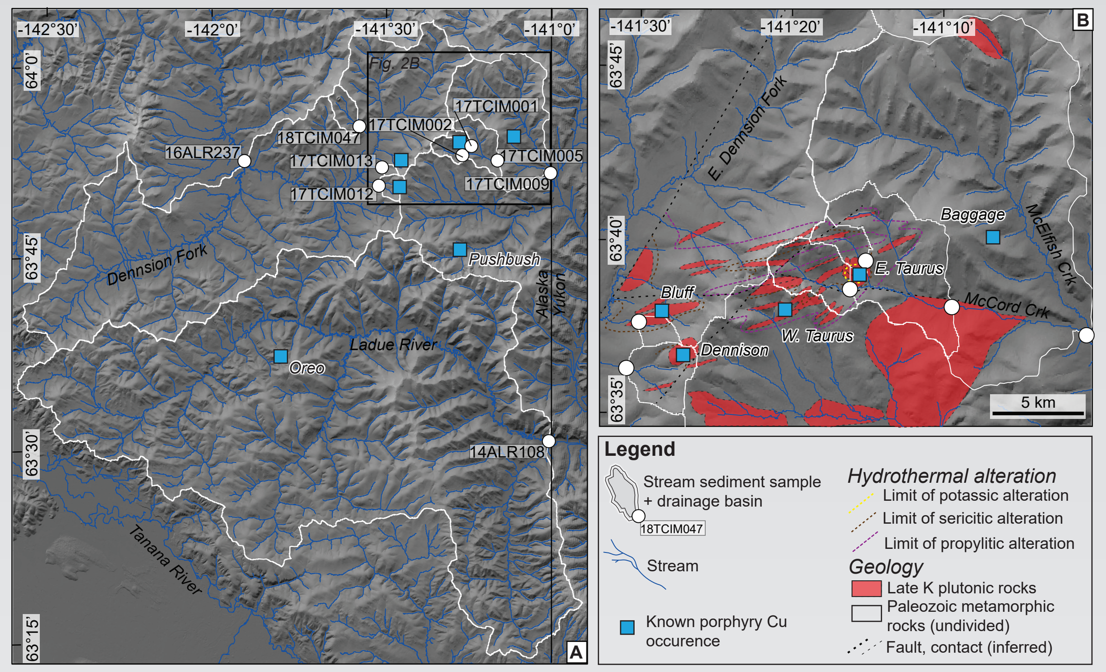

Figure 2: Geology of the Taurus porphyry Cu-Mo-(-Au) deposit and envircons and sample locales. (A) Stream sediment samples and associated drainage basins with regional porphyry deposits. (B) Detail of Taurus, Dennison, and Bluff mineralization centers. Alteration limit mapping after Kreiner et al. (2023). Limits of Late Cretaceous plutons after Wilson et al., 2015.

Takeaway: Stream sediment samples from sites at increasing distance from Taurus porphyry Cu-Mo(-Au) and associated mineralization centers.

Magnetite geochemistry measured by EPMA, microextures and inclusions characterized by SEM-EDS

Samples subject of hydrogeochemistry and indicator mineral work (Kelley and Graham, 2020; Kelley et al., 2021)

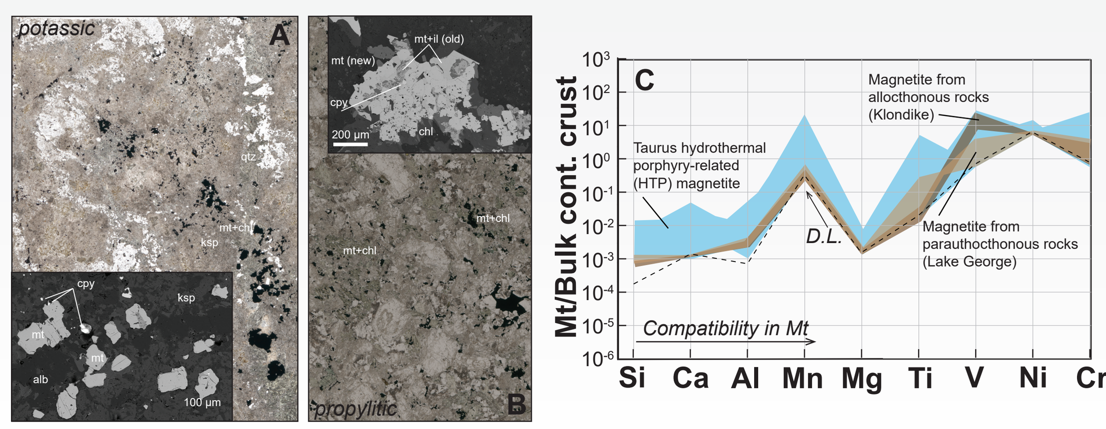

Figure 3: Taurus hydrothermal porphyry-related (HTP) magnetite. (A) Photomicrograph (PPL) of potassic alteration with magnetite accompanying K-feldspar overgrowths (see BSE inset). (B) Photomicrograph of propylitic alteration (PPL). BSE inset shows growth of new magnetite along with chlorite (chl) and chalcopyrite (cpy) inclusions. (C) Multi-element diagram of HTP (blue) and metamorphic (brown, beige) magnetite trace and minor elements measured by EPMA. D. L.-detection limit. Adapted from Dare et al., 2014.

Takeaway: Hydrothermal (HTP) magnetite abundant and exhibits unique geochemical signature

3. Detrital magnetite populations

Principal component analysis and Gaussian mixture modeling

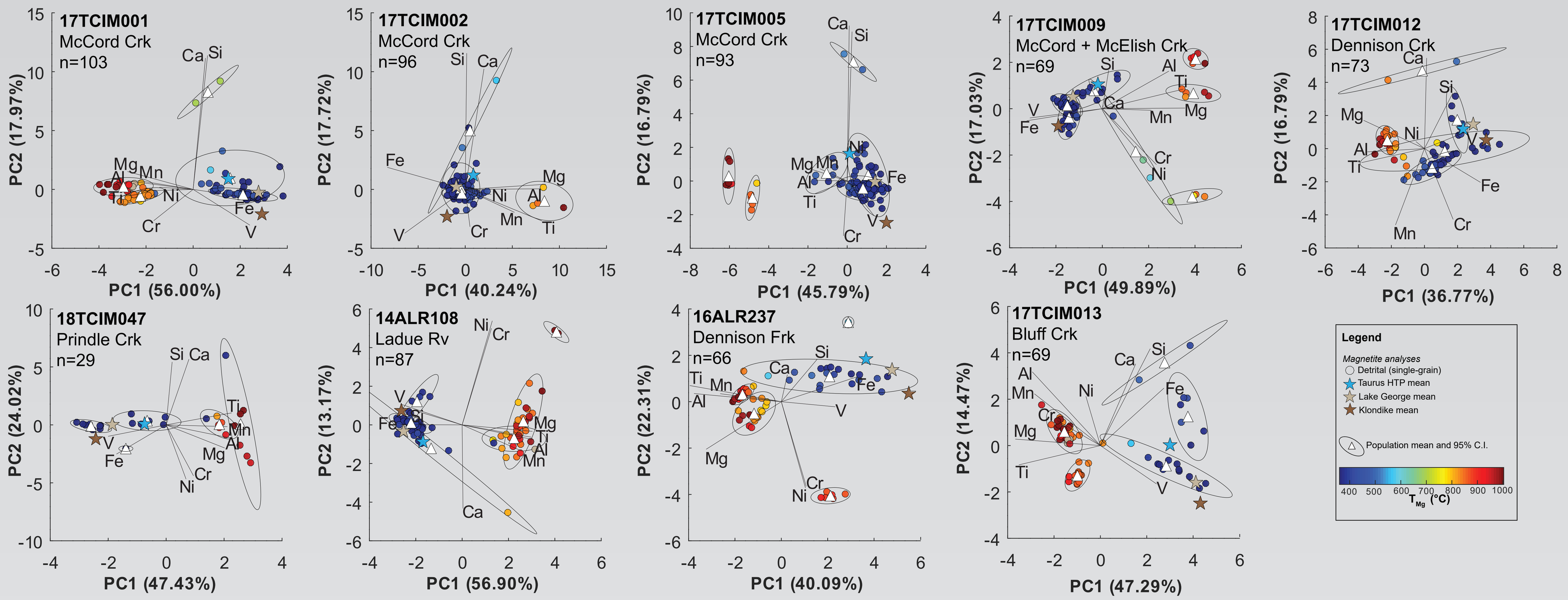

Figure 4: Principal component analysis of detrital magnetite EPMA data. Bi-plots for each sample (see Fig. 2) show standardized geochemical composition for each grain projected onto first and second principal components (% total variance explained by each component denoted in axis label). Individual points color-coded by Mg-in-magnetite (T_{Mg}) temperature (Canil and Lacourse, 2020). Superimposed vector length and angle are proportional to the influence of each variable on principal components. Results of Gaussian mixture modeling shown as population mean (white triangles) and 95% confidence interval. Stars mark mean geochemical composition of analyzed bedrock sources (see Fig. 3C) transformed into same space defined by detrital grains.

Takeaway: Geochemistry resolves at least 10 magnetite populations across sample set, some of which are compatible with known bed-rock sources (including Taurus-like HTP magnetite)

Interpretation of geochemical populations

Takeaway: Discriminant diagrams identify (1) igneous magnetite (TMg>650 °C) populations of variable composition, and (2) multiple hydrothermal populations compatible with porphyry Cu origin (note color-coding by inferred population from Fig. 4)

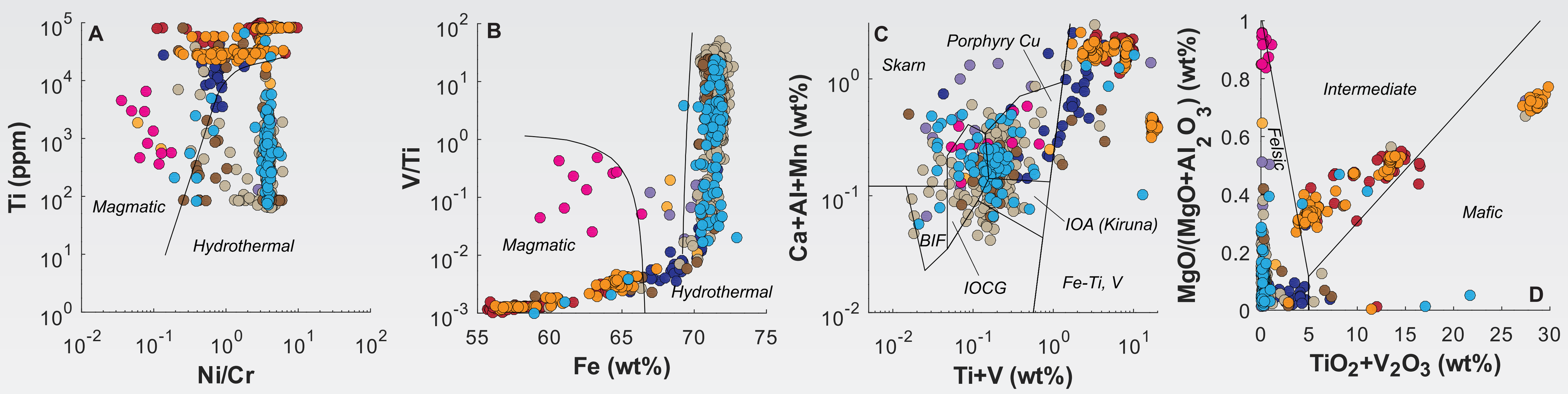

Figure 5: Magnetite geochemical discriminant diagrams. (A, B) Discrimination plots for hydrothermal versus magmatic magnetite (after Dare et al., 2014 and Wen et al., 2017, respectively. (C) Discriminant plot for magnetite from different ore deposit types (after Dupuis and Beaudoin, 2011). (D) Discriminant plot for igneous magnetite by composition (after Grigsby, 1990).

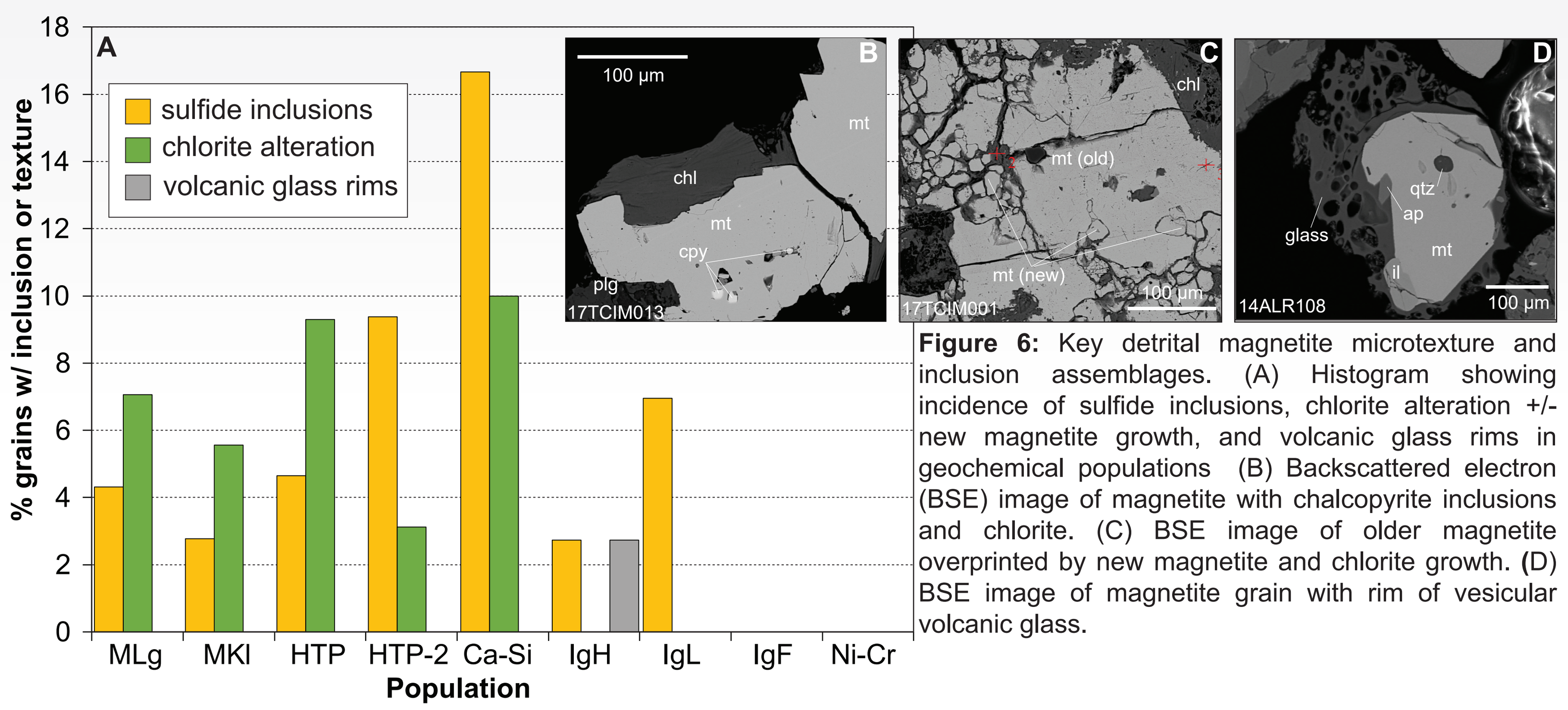

Figure 6: Key detrital magnetite microtexture and inclusion assemblages. (A) Histogram showing incidence of sulfide inclusions, chlorite alteration +/- new magnetite growth, and volcanic glass rims in geochemical populations (B) Backscattered electron (BSE) image of magnetite with chalcopyrite inclusions and chlorite. (C) BSE image of older magnetite overprinted by new magnetite and chlorite growth. (D) BSE image of magnetite grain with rim of vesicular volcanic glass.

Takeaway: Microtexture and inclusion assemblages support and refine inferences from geochemistry

Sulfide inclusions and/or chlorite alteration have elevated incidence of sulfide inclusions and/or chlorite and new magnetite growth

Volcanic glass rims in highest temperature volcanic glass rims support inference of igneous magnetite

4. Magnetite provenance patterns

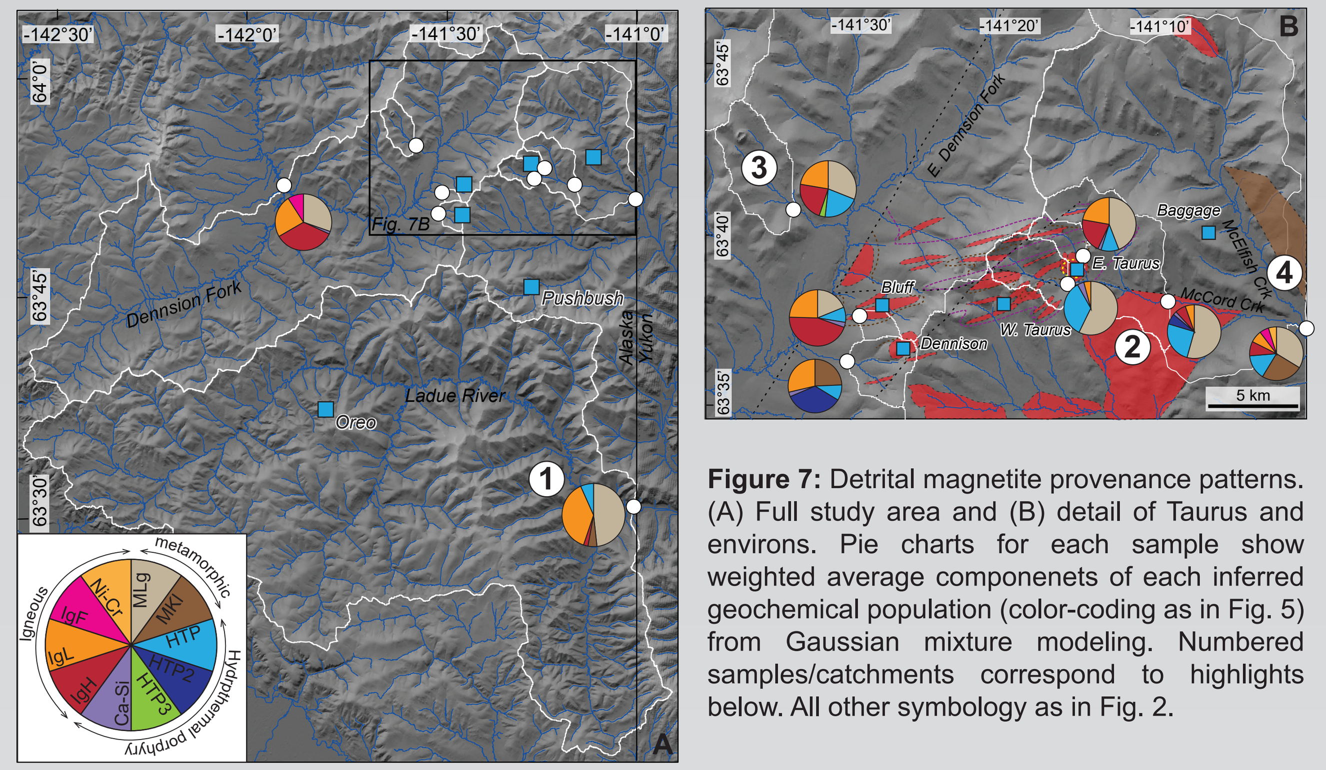

Figure 7: Detrital magnetite provenance patterns. (A) Full study area and (B) detail of Taurus and environs. Pie charts for each sample show weighted average components of each inferred geochemical population (color-coding as in Fig. 5) from Gaussian mixture modeling. Numbered samples/catchments correspond to highlights below. All other symbology as in Fig. 2.

1. Detrital magnetite with geochemical signature similar to Taurus HTP detected ~40 km downstream from known mineralization (14ALR108)

2. Proportion of HTP detrital magnetite decreases systematically downstream from Taurus mineralization center (17TCIM001-009)

3. HTP magnetite identified where no reported mineralization, but where prior work (Kelley and Graham, 2021) shows elevated B, Cu, Mn, and sulfate in surface water samples (18TCIM047)

4. Sample downstream (17TCIM009) of the confluence between McElfish and McCord Crks has detrital magnetite with charcateristic Klondike signature, whereas samples upstream do not, mirroring geologic map patterns

5. Magnetite (U-Th)/He analyses

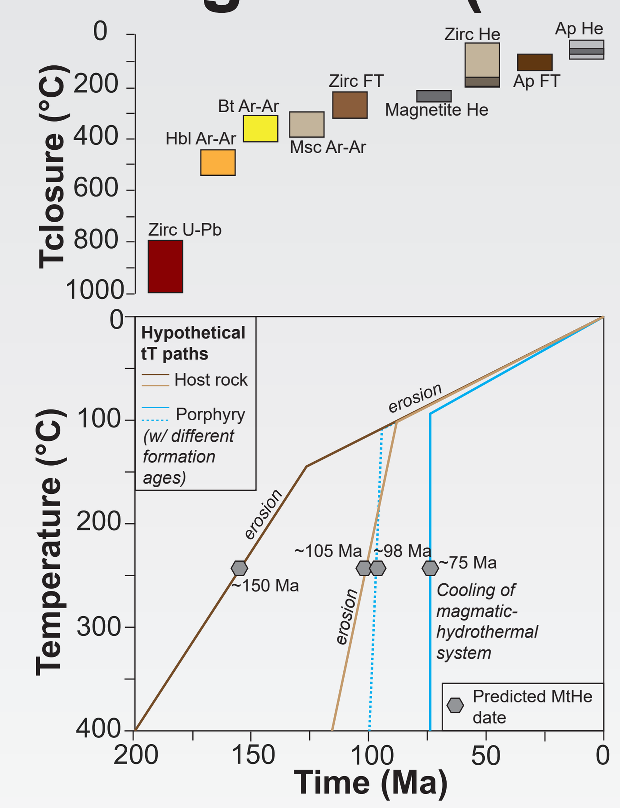

Figure 8: Magnetite (U-Th)/He thermochronometry. (A) Closure temperatures of magnetite (U-Th)/He and other common geo/thermochronometers. After Reiners and Brandon (2006) and Blackburn et al. (2007). (B) Hypothetical thermal histories and predicted magnetite (U-Th)/He dates for different detrital populations.

Takeaway: Magnetite from each geochemical population isolated for (U-Th)/He dating

Ongoing, but potential to inform the timing and/or exhumation of magnetite sources

6. Conclusions

Detrital magnetite geochemistry, textures, and inclusion assemblages fingerprint upstream (non)mineralized bedrock

U-Th)/He data (ongoing!) may add geologic context

Acknowledgements Funding for this research was provided by the U.S. Geological Survey Mineral Resources Program. We thank Karen Kelley and Richard Lease for providing sand samples analyzed in this study. EPMA performed at the Advanced Instrumentation Laboratory at the University of Alaska Fairbanks. SEM observations were collected in the Alaska Tephra Lab at the U.S. Geological Survey's Alaska Volcano Observatory in Anchorage, AK.

References (1) Canil & Lacourse, (2020). Chemical Geology, 541, 119576. (2) Blackburn et al., (2007). EPSL. (3) Dare et al. (2014). Mineralium Deposita (4) Dupuis & Beaudoin (2011). Mineralium Deposita. (5) Grigsby (1990). Journal of Sedimentary Research, (6) Kelley & Graham (2021), Applied geochemistry (7) Kelley et al. (2022). Ore Geology Reviews, 105021. (8) Kreiner et al. (2020), Canadian Institute of Mining and Metallurgy, Special Volume 57, (9) Kreiner et al. (2023). Economic Geology. (10) Murphy et al. (2006), Geological Association of Canada, Special Paper 45. (10) Reiners and Brandon (2006). Annu. Rev. Earth Sci. (11) Wen et al. (2017). Geochimica et Cosmochimica. Acta.